Investigation of the physico-chemical state and aggregation mechanism of surface Cr species on a Phillips CrO_x/SiO_2 catalyst by XPS and EPMA

Boping Liu, Minoru Terano*

School of Materials Science, Japan Advanced Institute of Science and Technology, 1-1 Asahidai, Tatsunokuchi, Ishikawa 923-1292, Japan

Abstract

X-ray photoelectron spectroscopy (XPS) and electron probe microanalysis (EPMA) were jointly applied to achieve some basic understandings of the physico-chemical state and aggregation mechanism of surface Cr species on an industrial Phillips CrO_x/SiO_2 catalyst calcined in dry air at 800°C for 20 h with 0.4 Cr/nm^2. The XPS results showed the coexistence of surface-stabilized hexavalent chromate species (70.4% expressed as $Cr(VI)O_{x,\,surf}$) and trivalent chromium oxide (29.6%) on the catalyst. The latter derived from calcination-induced reduction of the $Cr(VI)O_{x,\,surf}$ species is mostly chemically-bonded to the silica surface (expressed as $Cr(III)O_{x,\,surf}$). The EPMA map and line curves of the Cr distribution state on the catalyst revealed a small amount of the trivalent chromium oxide existed as a few aggregates in sizes of 200–300 nm on the surface of each particle, which were supposed to be crystallized aggregates of Cr_2O_3. Consequently, the calcination-induced reduction of $Cr(VI)O_{x,\,surf}$ to $Cr(III)O_{x,\,surf}$ species and the formation of Cr_2O_3 microcrystals on the Phillips catalyst with relatively low Cr loading were specifically confirmed. The variation of distribution and oxidation states of surface Cr species for the catalyst after being further calcined at 800°C for 2 h in the presence of moisture had also been studied in terms of the role of moisture and effect of atmosphere (pure air or N_2). It was found that the purposely introduced moisture induced the transformation of all the $Cr(III)O_{x,\,surf}$ and one-seventh of $Cr(VI)O_{x,\,surf}$ species into aggregates of Cr_2O_3 at high temperature, whereas oxidizing and inert atmospheres made no obvious difference. Finally, the formation mechanism of aggregates of Cr_2O_3 induced by moisture through cleavage of $Cr(III)O_{x,\,surf}$ species during the calcination had been speculated considering of the indispensable evolution of traces of moisture from the simultaneous dehydroxylation of residual hydroxyl groups on silica surface. The advantages of the combination of XPS and EPMA techniques for the basic investigation of Phillips catalysts were substantiated by the results obtained in this study. © 2001 Elsevier Science B.V. All rights reserved.

Keywords: Phillips CrO_x/SiO_2 catalyst; Surface Cr species; Aggregation; Electron probe microanalysis; X-ray photoelectron spectroscopy

1. Introduction

As one of the most important members in the family of commercial polyolefin catalysts, Phillips catalyst is still responsible for several million tons of commercial production of polyolefins including HDPE and LLDPE, etc. In spite of more than 40 years of research efforts, since its discovery by Hogan and Banks in the early 1950s, many aspects concerning the physico-chemical state of the surface Cr species as well as the polymerization mechanism still remain controversial [1–9]. The phsico-chemical

* Corresponding author. Tel.: +81-761-51-1620;
fax: +81-761-51-1625.
E-mail address: terano@jaist.ac.jp (M. Terano).

state of surface Cr species, which is closely related to the molecular structure, texture and orientation of the chromium oxide on the catalyst surface, seems playing crucial roles for a deeper understanding of the Phillips catalyst [1–4,9]. In the literature, many different methods, such as oxygen chemisorption [10–12], magnetic susceptibility measurement [13,14], XRD [15–18], EPR [14,19,20], SIMS [21], Raman [17,22–24], UV–VIS DRS [14,19,22], EXAFS-XANES [25], PIXE [26], TPR [8,18,19], SEM/EDS [27], IR [8,28] and XPS [8,17,26,29–42], etc. had been used separately or jointly to characterize the physico-chemical state of Cr species on Phillips catalysts. It was generally accepted that the bulk CrO_3 could be highly dispersed and stabilized as surface chromate species (i.e. monochromate and dichromate, sometimes even polychromate) through the reaction with the surface groups on silica gel during the calcination process at 300–900°C in oxygen or dry air [4,15,32,43]. Usually, a highly dispersed state of surface-stabilized chromate species can be achieved through many redispersion cycles of sublimation, volatilization, spreading, deposition and stabilization of bulk CrO_3 (mp 196°C and bp 250°C) on the support surface during the calcination [4,5]. Whereas there are two frequently reported unfavorable phenomena occurred during the calcination process: the calcination-induced reduction of surface-stabilized hexavalent chromate species into lower valent state (+5, +4 or +3) [10–14,19,26,32,44–46] and the creation of aggregated Cr_2O_3 (usually in crystallized form) [4,15,18,23,31,43,47], although an oxidizing atmosphere (O_2 or dry air) is utilized. These affect in a great extent the physico-chemical state of the surface Cr species, thus the properties and performance of the catalyst. Especially the formation of Cr_2O_3 crystallites (mp 2435°C and bp 4000°C), which was highly stable and thought to deactivate the catalyst for ethylene polymerization, may occur at any stage of the catalyst preparation: calcination, reduction and activation, or even during the polymerization process [4,18,19,20]. As a result, the supported Cr species may be present on the silica surface in a mixture of different valence, coordination and distribution states, depending on the preparation conditions [26–31,34,35]. For a catalyst in calcined form, the main factors which affect the calcination-induced reduction and the appearance of the undesirable aggregated Cr_2O_3

include the Cr loading, calcination temperature, calcination duration, type of support, gas media, etc. Furthermore, there is a limitation of the dispersion and stabilization of chromium oxide on support surface, i.e. saturation coverage, which is proportional to the surface hydroxyl density, surface area of the support and inversely proportional to the calcination temperature [4,15,43]. When the content of the CrO_3 exceeds the saturation coverage under a given condition, the excess of CrO_3 decomposes into aggregated Cr_2O_3 on the support surface during calcination [4,15,23,31,43,47].

In this work, our interests will be mainly focused on the following two unclear questions concerning the physico-chemical state of surface Cr species on a calcined Phillips CrO_x/SiO_2 catalyst with relatively low Cr loading ca. 0.4 Cr/nm^2 (i.e. 1 wt.% Cr for silica with 280 m^2/g, much lower than the saturation coverage for silica [15,43]), where the Cr loading of an industrial catalyst usually locates. The first ambiguous question is, weather the formation of aggregated Cr_2O_3 occurs or not even under this relatively low Cr loading. It is usually beyond the sensitivity limitation of the measurement for detecting the occurrence of aggregates under this low Cr loading by most of the conventional spectroscopy methods [8]. Therefore, Some disputes concerning this topic are still in existence due to the lack of direct and conclusive evidences. For example, Ellison and coworkers [21,25] found that clustering of Cr species even occurred on CrO_x/SiO_2 catalysts (525–600°C in air, 350 m^2/g) with 1 wt.% Cr from SIMS as well as EXAFS-XANES characterization. According to the report of Cimino et al. [29], when a Phillips CrO_x/SiO_2 catalyst (300–700°C in air for 5 h, 210 m^2/g) with 1 wt.% Cr was calcined over 600°C the formation of agglomerated Cr_2O_3 was detectable by XRD method. Whereas Zaki et al. [22] reported that the α-Cr_2O_3 detection on Phillips CrO_x/SiO_2 catalysts (300–600°C in air for 5 h, 210 m^2/g) was beyond the sensitivity of the XRD technique when the Cr loading was lower than 3 wt.%. Recent results of Wang and Murata [16] who used a CrO_x/SiO_2 catalyst (700°C in air for 3 h) indicated that the XRD method was unable to detect the formation of Cr_2O_3 when the Cr loading was below 2 wt.%, while the Cr_2O_3 aggregates most probably already existed as they suggested. On the other hand, some Raman studies by Wachs and coworkers [23,48–50] on calcined Phillips CrO_x/SiO_2

catalysts (500°C for 16 h or 700°C for 2 h, 300 m^2/g) with Cr loading from 0.1 to 2 wt.% did not show the presence of crystalline Cr$_2$O$_3$. McDaniel [15] studied the calcination mechanism of CrO$_x$/SiO$_2$ catalysts (200–800°C in air for 18 h, Davison 952/280 m^2/g) with 1.5 or 3 wt.% Cr and found that only Cr^{6+} was found up to 600°C, but at 800°C some decomposition of hexavalent Cr to lower valence states was noticed, particularly at 3 wt.%, XRD indicated the formation of Cr$_2$O$_3$ crystallites in diameter of 40 nm. Bensalem and Weckhuysen et al. [20] confirmed the absence of Cr$_2$O$_3$ clusters for a CrO$_x$/silica (400°C in O$_2$ for 2 h, 800 m^2/g) catalyst with 0.5 wt.% Cr by EPR. Jóźwiak and Lana [18] even reported that ground crystalline α-Cr$_2$O$_3$ could be completely oxidized, dispersed and stabilized as chromate species on silica (165 m^2/g) at low Cr loading ca.0.5 wt.% after calcination in O$_2$ or dry air up to 700°C from their XRD and TPR evidence. Some researchers only supposed the possibility of creating Cr$_2$O$_3$ microcrystals in a separate reduction step on a CO [20,27,51] or H$_2$ [19] reduced Phillips catalyst with relatively low Cr loading. The discrepancy mentioned above may be derived from the diversity of the catalyst preparation conditions and the difference in sensitivity of the analytical methods. Supposing the clustering and formation of aggregated Cr$_2$O$_3$ could be confirmed on a Phillips CrO$_x$/SiO$_2$ catalyst with relatively low Cr loading ca.0.4 Cr/nm^2, the second confusing question would be what is the origin and formation mechanism of this aggregated Cr$_2$O$_3$. Previously, the formation of aggregated Cr$_2$O$_3$ is usually thought to be related with the thermal decomposition (or reduction) of bulk CrO$_3$ [4,15,18,23,31,43,47], but this seems unreasonable when the Cr loading is much lower than the saturation coverage. It is also supposed to be significantly affected by the presence of moisture [14,18,29,43,47] and O$_2$ concentration [43] in the calcination gas media. Nevertheless, the specific mechanism has seldom been dealt with before. Especially the relationship and difference between the calcination-induced reduction of surface chromate species and the thermal decomposition (or reduction) of bulk CrO$_3$ has never been discussed, in which the former may also play some roles in formation of aggregated Cr$_2$O$_3$. Bearing these questions in mind, the surface analytical methods XPS and EPMA, which can obtain the substantial information of the oxidation and distribution states of

surface Cr species, are considered for characterization of the catalyst implemented in this work.

In our previous research, a better understanding of the oxidation and distribution states on several titanium-based Ziegler–Natta polyolefin catalysts had been achieved by XPS [52–55] and SAM [55–57] methods. The XPS is also a powerful method for measuring the oxidation state of Cr on Phillips catalysts [8,17,26,29,30–42]. The binding energy (BE) of the Cr 2p level is frequently used as a criterion for identifying the oxidation state of the surface Cr species. On the other hand, the full width at half maximum (FWHM) value of the Cr 2p spectrum is a reflection of the distribution state of the Cr species in its corresponding oxidation state, which also give valuable information especially for discriminating aggregated Cr$_2$O$_3$ from surface-stabilized and highly dispersed Cr species. Both qualitative and quantitative information of surface Cr species in mixed oxidation states can be obtained by XPS method [26,28–31,34,35,42]. Two surface analytical methods PIXE and SEM/EDS has been used to directly map the distribution state of surface Cr species on Phillips catalysts before by Rahman et al. [26] and Schmidt et al. [27], respectively, but they just got the Cr images at relatively low resolution from different catalysts(CrO$_x$/Al$_2$O$_3$ and CO-reduced CrO$_x$/SiO$_2$, respectively) at relatively high Cr loading (4.4–5 wt.%). The SAM is also not practical for mapping the distribution state of Cr due to too small difference of the Auger electron peak energy between Cr (525 eV) and O (503 eV). The EPMA method with high resolution makes it possible to directly map the distribution state of the Cr species on a Phillips catalyst with relatively low Cr loading. In general, our approach is based on the XPS technique combined with EPMA measurements for study of the physico-chemical state and formation mechanism of aggregated Cr$_2$O$_3$ on an industrial Phillips CrO$_x$/SiO$_2$ catalyst with 0.4 Cr/nm^2 of Cr loading.

2. Experimental

2.1. Catalyst and treatments

Nitrogen (B-grade, impurity <5 ppm) and pure air (S-grade, impurity <1 ppm) purchased from Uno Sanso Co., were used directly without further

purification. Commercial bulk CrO_3 and Cr_2O_3 were bought from Wako Pure Chemical Industries Ltd., and Kanto Chemical Co., Inc., respectively. A Phillips CrO_x/SiO_2 catalyst (S-1) was donated by Japan Poly-olefin Co., Ltd., which was prepared from impregnation of Davison 952 silica gel (BET surface area ca. $280\, m^2/g$) with aqueous solution of CrO_3 followed by calcination in dry air up to $800°C$ for 20 h. The catalyst was stored in small glass ampoule bottles sealed under nitrogen atmosphere before use. The chromium content of the catalysts was ca. 1 wt.% (i.e. $0.4\, Cr/nm^2$). The ethylene polymerization activity of this catalyst was confirmed to be similar with that in its commercial production line. Other two samples (S-2 and S-3) were prepared from treatments of the catalyst (S-1) at $800°C$ for 2 h in moisture-contained pure air flow (S-2) and moisture-contained N_2 flow (S-3), respectively, in a quartz microreactor. The pure air or nitrogen flow was bubbling through a glass vessel filled with pure water before entering into the microreactor.

2.2. Sample characterization

2.2.1. The XPS instrumentation

The XPS data were obtained on a Physical Electronics Perkin-Elmer Model Phi-5600 ESCA spectrometer with monochromated Al Kα radiation (1486.6 eV) operated at 300 W. Each sample was embedded on a conductive copper tape to form a sample disc in a diameter of 5 mm and fixed on a sample holder. The sample holder was then put into the vacuum transfer vessel (Phi Model 04-110, Perkin-Elmer Co., Ltd.), which can be connected to the sample introduction chamber on the XPS instrument for sample transfer without atmospheric exposure. The above procedures were carried out in a glove bag, which had been purged overnight with nitrogen gas in advance. The prepared sample was degassed in the introduction chamber to 10^{-7} Torr before entering the main chamber, in which the vacuum was kept above 5×10^{-9} Torr during XPS data acquisitions. A neutralizer was used to reduce the charging effect to obtain a better signal to noise ratio. The difficulty in XPS study of a Phillips catalyst is to minimize the X-ray induced reduction during the XPS measurements. The X-ray induced reduction during XPS acquisition was found to be significantly dependant on the preparation conditions of the catalyst. The

partially thermal-reduced catalyst implemented in this study was found to be only slightly affected by the X-ray irradiation during the XPS measurement within 2 h. This agrees well with the report of Best et al. who also investigated a partially thermal-reduced Phillips catalyst using a monochromated X-ray source [31]. All XPS spectra for oxidation state determination of Cr were obtained within 2 h (if not specified) with only negligible X-ray induced reduction to the surface Cr species. All binding energies were referenced to the Si 2p peak of silica gel at 103.3 eV to correct for the charging effect during acquisition [38]. Another challenging problem confronted is a precise multiplet fitting of the Cr 2p level in a mixed oxidation states. To pursue this, the bulk CrO_3 and Cr_2O_3 were also measured together with some literature data for Phillips catalysts in single "pure" oxidation state [32] as references for XPS data analysis. Multiplet fittings of the Cr 2p XPS curves by the Gaussian–Lorentzian method were carried out to determine the mixed states of valences in all the samples. The fitting for each curve was repeated for several times to ensure a reproducible result.

2.2.2. EPMA measurements

The EPMA measurements were carried out on a JEOL JXA-8900L system. At first, the door of the sample transfer chamber was covered with a glove bag, in which nitrogen was purged overnight to remove impurities including traces of moisture and oxygen. A double spreading carbon tape specially made for electron microscopy by Japan Oken Co., Ltd., was used as a conducting substrate to fix the catalyst sample. Each catalyst sample was embedded on the carbon tape and fixed on the sample holder in the glove bag under nitrogen atmosphere. Finally, the sample holder was put into the sample transfer chamber, by which the sample could be introduced into the measuring chamber without atmospheric exposure. The vacuum in the EPMA main chamber was typically under 1×10^{-5} Torr. The EPMA was used with an accelerating voltage of 20 kV, a probe current of 2×10^{-8} A and a probe electron beam diameter of 1 μm. Dispersive crystal of TETJ was used for wavelength dispersive X-ray analysis (WDX). Both map and line analyses of Cr were carried out for characterization of the distribution state of Cr species on the catalyst surface. The surface roughness of the catalyst particle would slightly

affect the relative intensity of the Cr signal (the convex surface leading to slightly higher Cr intensity) without changing the main characteristic of the Cr distribution state. For characterization of each catalyst sample, the distribution states of Cr on many different catalyst particles of the same sample were carefully observed to get the most typical and reproducible results.

3. Results and discussion

3.1. The oxidation and distribution states of Cr on the Phillips catalyst

As a fundamental aspect for making a precise and proper prediction of the oxidation state of surface Cr species on the supported catalyst, some XPS measurements were carried out on pure chromium oxides to obtain Cr 2p spectra (shown in Fig. 1) in mixture with small amount of silica as reference. The Cr 2p region of silica without Cr supporting (not shown) was also measured, which facilitated the base line determination for the Cr 2p spectra during fitting treatment [38]. The BE and FWHM values from Cr 2p(3/2) level of bulk CrO_3 and Cr_2O_3 were listed in Table 1 together with a comparison with those from [29,30,32,41]. As it can be seen, the deviation of BE values from Cr 2p(3/2) level of bulk chromium oxides in Table 1 mainly generated from the reference peak for charging effect correction for different researchers. For example, Cimino et al. [29] used the value of 283.8 eV of the C 1s level resulting from the contaminated carbon as reference, whereas Okamoto et al. [30] took the same C 1s reference at 1.2 eV higher (i.e. 285.0 eV) for correction. This can explain why the former got the lower BE value. Our results of Cr 2p(3/2) level for CrO_3 (BE: 579.24 eV, FWHM: 2.53 eV) and Cr_2O_3 (BE: 576.59 eV, FWHM: 3.03 eV) seem reasonable and very near to the average values in Table 1 after correction using the same reference of Au 4f(7/2) = 84 eV or C 1s = 285 eV. From Table 1 and Fig. 1, one can find the most pronounced feature of Cr 2p peak for bulk chromium oxides compared with the supported Cr-based catalyst is the small FWHM values, so to speak the sharp peak morphology, which will be utilized as an important reference for discriminating aggregated Cr_2O_3 from surface-stabilized and highly dispersed Cr species in the later discussion.
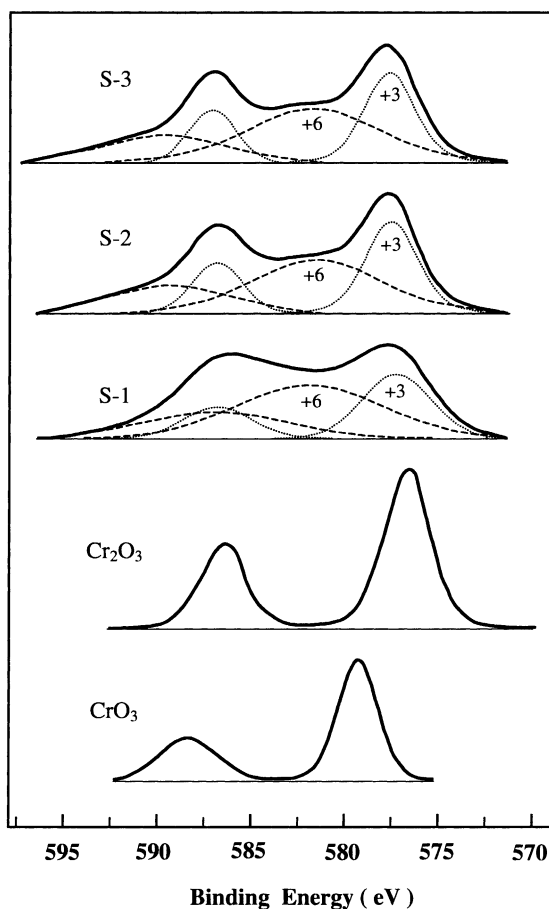

Fig. 1. The XPS spectra of Cr 2p level for CrO_3, Cr_2O_3, the Phillips CrO_x/SiO_2 catalyst (S-1) and the two thermal-treated samples (S-2 and S-3) from S-1.

Fig. 1 also showed the XPS spectra of Cr 2p level for the industrial Phillips CrO_x/SiO_2 catalyst (S-1) in calcined form. A single doublet fitting for this spectrum was found to be impossible for getting a perfect curve fitting, which indicated that a mixed oxidation states existed in this catalyst. This also means the Phillips catalyst (S-1) had suffered calcination-induced reduction and/or thermal decomposition during the thermal-treatment at 800°C for 20 h in its preparation process leading to the formation of some surface Cr species in a lower oxidation state. A multiplet fitting was applied and its corresponding BE and FWHM values of Cr 2p(3/2) level was tabulated in Table 2. Two oxidation states were found in this

Table 1
The XPS data from fitting of Cr 2p spectra for bulk chromium oxides

Chromium oxide	Reference	Cr 2p(3/2)		Reference peak
		BE (eV)	FWHM (eV)	
CrO$_3$	This work[a]	579.24	2.53	Si 2p, 103.3 eV
	[32]	579.1	2.9	Au 4f, 84 eV
	[30]	580.3	2.8	C 1s, 285 eV
	[29]	578.7	1.6	C 1s, 283.8 eV
	[41]	577.1	2.3	Au 4f, 82.8 eV
Average value[b]		579.37	2.43	
Cr$_2$O$_3$	This work[a]	576.59	3.03	Si 2p, 103.3 eV
	[32]	576.2	3.5	Au 4f, 84 eV
	[30]	576.6	3.6	C 1s, 285 eV
	[29]	575.6	3.0	C 1s, 283.8 eV
	[41]	575.6	3.0	Au 4f, 82.8 eV
Average value[b]		576.60	3.23	

[a] The XPS spectra were measured in mixture of bulk chromium oxides with small amount of silica gel as reference under high resolution acquisition mode within 10 min.

[b] The average BE values were obtained after correction using the same reference of Au 4f(7/2) = 84 eV or C 1s = 285 eV.

catalyst namely the first with a BE of 581.81 eV and a FWHM of 9.62 eV assigned as an oxidation state of +6 (atomic concentration 70.4%) and the second with a BE of 577.21 eV and a FWHM of 4.43 eV assigned as an oxidation state of +3 (atomic concentration 29.6%). Accordingly, almost one thirds of the hexavalent Cr species was subject to calcination-induced reduction (from chromate species) and/or thermal decomposition (from bulk CrO$_3$) during calcination. The next important aspect is to determine the real physico-chemical state of this two kinds of Cr species in oxidation states of +6 and +3, respectively, on the silica surface: chemically stabilized or in bulk phase?

The BE value of 581.81 eV for the surface Cr species in an oxidation of +6 on the calcined catalyst is 2.57 eV higher than that of 579.24 eV for the bulk CrO$_3$. The shifting in Cr 2p(3/2) BE demonstrated that this surface Cr is surface-stabilized chromate species (including monochromate, dichromate and sometimes even polychromate expressed as Cr(VI)O$_{x,\,surf}$). Such an increase in BE is acceptable when the Cr species becomes isolated on the silica gel with weak acidity,

Table 2
The XPS data from multiplet fitting of Cr 2p spectra for the Phillips CrO$_x$/SiO$_2$ catalyst (S-1) and two thermal-treated samples (S-2 and S-3) from S-1[a]

Sample	Cr 2p(3/2)		Valent state assignment	Atomic percentage[b] (%)	Relative intensity of Cr 2p peak[c]
	BE (eV)	FWHM (eV)			
S-1	581.81	9.62	+6	70.4	3.8
	577.21	4.43	+3	29.6	
S-2	581.64	8.30	+6	59.4	2.6
	577.58	3.28	+3	40.6	
S-3	581.74	8.30	+6	60.8	2.7
	577.64	3.26	+3	39.2	

[a] The XPS measurements were carried out under high resolution acquisition mode within 2 h.

[b] Percentage of the fitted peak areas of each valence component versus the whole area of Cr 2p spectrum.

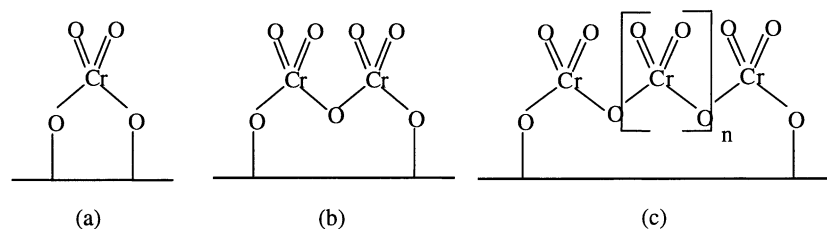[c] Using the calculation method of [32].

Fig. 2. Plausible structures of surface-stabilized hexavalent chromate species $(Cr(VI)O_{x, surf})$ on silica surface of the Phillips CrO_x/SiO_2 catalyst ($n \geq 1$).

since the electron extracting effect from the oxygen atoms on silica gel is stronger than it would be in the CrO_3 lattice [32]. This effect could be further strengthened by the increasing strain in the surface siloxane groups due to the successive dehydroxylation upon calcination [4,15]. This is favorably supported by the experimental evidence reported by Thüne et al. [38] and Merryfield et al. [32]. The former got a BE of 581.3 eV (reference: Si 2p = 103.3 eV) for a model $Cr(VI)O_x/SiO_2/Si(1\,0\,0)$ catalyst with 1 Cr/nm^2 calcined in He/O$_2$ at 450°C within 1 h. The latter obtained BE values (reference: Si 2p = 103.5 eV) of 581.6 eV (FWHM = 3.7 eV) and 581.7 eV for $Cr(VI)O_x/SiO_2$ catalysts with 0.4 Cr/nm^2 and 1.2 Cr/nm^2, respectively, prepared upon calcination in dry air at 650°C for 1 h. The lower calcination temperature and much shorter calcination time account for their no occurrence of calcination-induced reduction and/or thermal decomposition resulting in catalysts in "pure" Cr oxidation state of +6. In our case, the higher calcination temperature and much longer calcination time most probably contributed to the formation of more polymerized chromate species in different polydispersities as well as the occurrence of calcination-induced reduction and/or thermal decomposition. The former was reflected from the FWHM value of 9.62 eV indicating much more heterogeneous physico-chemical state of our surface chromate species including the effect from its local environment of mixed oxidation states. The calcination mechanism of CrO_x/SiO_2 catalysts (200–800°C in air for 18 h) with 0.6 or 1.2 Cr/nm^2 was studied by McDaniel [15]. The molar ratio of reacted OH and Cr was found to decrease from two to even below one with increasing temperature, so he suggested that monochromate was initially formed followed with some possible

secondary formation of dichromate or even polychromate in the later stage of calcination. The coexistence of polychromate with monochromate and dichromate species on calcined Phillips CrO_x/SiO_2 catalysts had also been frequently reported by other researchers [14,19,22,23]. The specific molecular structures of the anchored chromate species $(Cr(VI)O_{x, surf})$ are not elucidated yet, and Fig. 2 just illustrates its plausible structures on the silica surface postulated in the literature [14,15,19,22,23]. Best et al. [31] got results of much lower Cr 2p(3/2) BE (579.9 eV) ascribed to the chromate species on CrO_x/SiO_2 catalysts (300–400°C in air for 4 h, silica: Cab-O-Sil grade M-5) with high Cr loading 8 wt.%. The most probable explanation is that they abtained measurements on a mixture of chromate species and bulk CrO_3 rather than chromate species solely, since their Cr loading was far above the saturation coverage [4,15,32,43].

As for the surface Cr species in an oxidation of +3 on this calcined catalyst, its BE value of 577.21 eV and FWHM value of 4.43 eV seem quite different from the typical values of the bulk Cr_2O_3. Especially the latter strongly suggests its surface-stabilized and highly dispersed characteristics, i.e. trivalent Cr species chemically bonded to silica surface $(Cr(III)O_{x, surf})$. This assignment is firmly supported by the work of McDaniel et al. [32], who prepared a standard surface-stabilized $Cr(III)O_x/SiO_2$ sample (from 300°C calcination of Cr(III) acetate on silica in wet N$_2$) with a BE value of 577.6 eV and a FWHM value of 4.9 eV for the Cr 2p(3/2) level. Compared with bulk Cr_2O_3, the higher BE of $Cr(III)O_{x, surf}$ species might be resulted from the stabilizing effect of the silica as well as the environmental effect of neighboring chromate species, and the larger FWHM value could be ascribed to its variety in molecule structure and the
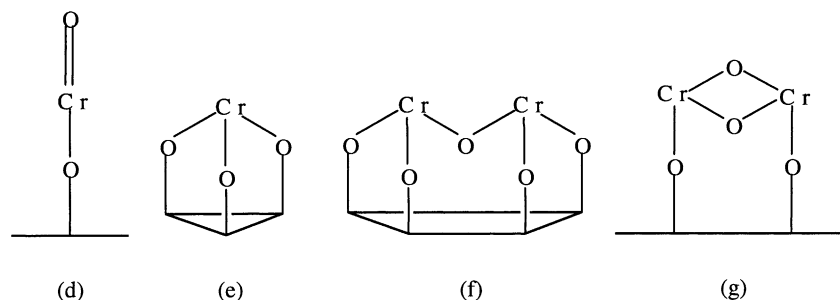
Fig. 3. Plausible structures of surface-stabilized trivalent chromium species $(Cr(III)O_{x,\,surf})$ on silica surface of the Phillips CrO_x/SiO_2 catalyst.

heterogeneity of the silica surface. The appearance of surface-stabilized $Cr(III)O_{x,\,surf}$ species on Phillips catalysts had been frequently reported by other researchers [10–14,19,26,32,44–46]. Although its specific molecular structure is still remained ambiguous, four plausible structure models (illustrated in Fig. 3) had been proposed before [14,44–46]. The formation of this $Cr(III)O_{x,\,surf}$ species was thought to originate from calcination-induced reduction of the chromate $Cr(VI)O_{x,\,surf}$ species and to increase with calcination temperature and time. This calcination-induced reduction is reasonable judging from the variation of state of the chromate $Cr(VI)O_{x,\,surf}$ species in the calcination process. As the calcination proceeds at high temperature, i.e. 800°C, the strain in the surface Si–O bonds developed by the successive dehydroxylation of hydroxyl groups, will become more and more dominant in affecting the chemical stability of the chromate species. Lower Cr loading means more hydroxyl groups are removed by dehydroxylation rather than by reaction with CrO_3 so as to create much stronger strain in the surface Si–O bonds. The shifting of the BE to higher value for the chromate $Cr(VI)O_{x,\,surf}$ species resulted from surface-stabilization effect and successive increasing strain in the surface siloxane group during calcination implies a decreasing electron density, i.e. an increasing reduction-potential. It can be expected that the calcination-induced reduction of the chromate $Cr(VI)O_{x,\,surf}$ to $Cr(III)O_{x,\,surf}$ species occurs at certain critical point depending on specific conditions including temperature, duration, etc. Jóźwiak and Lana [18] depicted such an image that the chromate $Cr(VI)O_{x,\,surf}$ species could suffer calcination-induced reduction through an oxygen

desorption process originating from its terminal Cr=O bonds and subsequently change into $Cr(II)O_{x,\,surf}$ species at 800°C in a neutral atmosphere. In our case, surface $Cr(III)O_{x,\,surf}$ species would be expected due to the much higher stability of $Cr(III)O_{x,\,surf}$ species than the $Cr(II)O_{x,\,surf}$ species in O_2-contained atmosphere [46]. One thing worth notice is the slightly lower BE and FWHM values of the Cr 2p(3/2) level for the $Cr(III)O_{x,\,surf}$ species on our catalyst compared with that of the standard $Cr(III)O_x/SiO_2$ sample by McDaniel et al. [32], which suggest the existence of a small amount of bulk Cr_2O_3 can not be completely excluded.

Fig. 4 shows the typical results of EPMA map and line curves of the Cr distribution on the calcined catalyst. As it can be seen, the Cr species mostly dispersed uniformly on the surface of each catalyst particle. This strongly support the above assignments to the surface Cr species on our catalyst namely the surface-stabilized, highly dispersed $Cr(VI)O_{x,\,surf}$ and $Cr(III)O_{x,\,surf}$ species. Whereas the heterogeneity of Cr distribution on each individual catalyst particle was also revealed in all the EPMA images measured on this catalyst, that is the existence of a few of local aggregates of Cr species in sizes of 200–300 nm on the surface of the catalyst. These aggregates corresponding to the red patches (marked in circles) in the map image and sharp peak in the line curves in Fig. 4(a) and (b), respectively, were supposed to be microcrystal particles of Cr_2O_3. With the aid of the combined techniques of XPS and EPMA, a clear image of the surface physico-chemical state on an industrial Phillips catalyst in calcined form is obtained, that is the existence of three kinds of surface Cr species
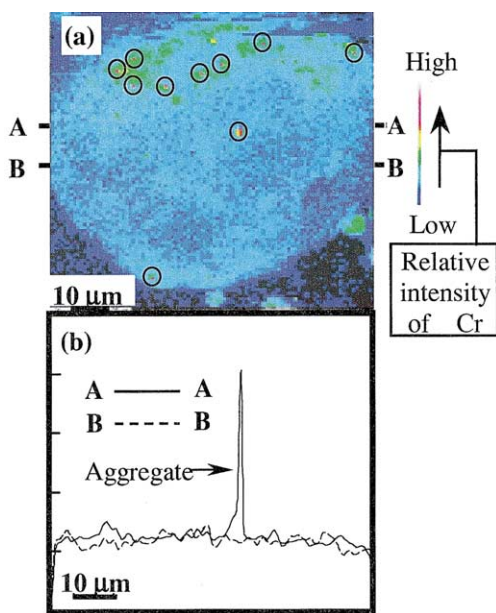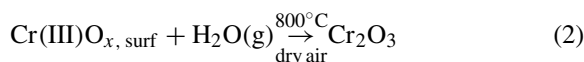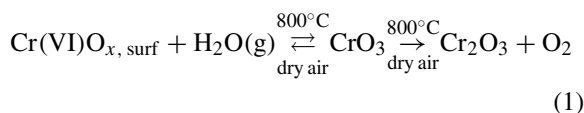
Fig. 4. The EPMA map (a) and line curves (b) of the chromium distribution on the Phillips CrO$_x$/SiO$_2$ catalyst. The line curves of A–A and B–B in (b) are corresponding to the chromium distribution at the straight-line positions of A–A and B–B in (a), respectively. The red patches marked in circles in (a) are corresponding to small aggregates of surface Cr species.

on our catalyst namely the Cr(VI)O$_{x,\,surf}$ chromate (ca. 70%) and Cr(III)O$_{x,\,surf}$ species (ca. 29%) and small amount of Cr$_2$O$_3$ microcrystals. Consequently, the calcination-induced reduction of Cr(VI)O$_{x,\,surf}$ to Cr(III)O$_{x,\,surf}$ species and the formation of aggregated Cr$_2$O$_3$ in a calcined Phillips catalyst with even relatively low Cr loading, i.e. 0.4 Cr/nm^2 were specifically confirmed. The second unavoidable question is what is the origin and formation mechanism of this aggregated Cr$_2$O$_3$, which cannot be simply explained by the "calcination-induced reduction" and/or "thermal decomposition". A detailed understanding of the origin and formation mechanism of the aggregated Cr$_2$O$_3$ is in great demand as for a state-of-art designing of this important industrial catalyst.
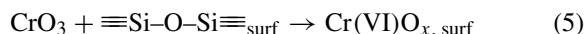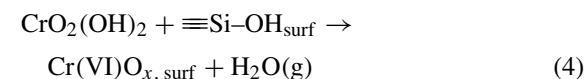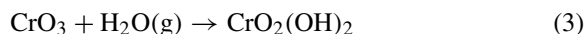
3.2. The oxidation and distribution states of Cr on the thermal-treated samples

According to previous reports [14,26,29,42], the formation of aggregated Cr$_2$O$_3$ on catalysts with

low level Cr loading usually occurs in the later stage of calcination behind the full stabilization of bulk CrO$_3$ as chromate species and a consequent calcination-induced reduction into Cr(III)O$_{x,\,surf}$ species. It is also supposed that the formation of aggregated Cr$_2$O$_3$ is significantly affected by the presence of moisture [14,18,29,43,47] and O$_2$ concentration [43] in the calcination gas media. In connection with the image of the surface physico-chemical state on our Phillips catalyst described in the previous section, two possible routes shown in Eqs. (1) and (2), respectively, should be taken into prior consideration for creation of aggregated Cr$_2$O$_3$ considering of the inevitable evolution of traces of moisture from the simultaneous dehydroxylation of residual hydroxyl groups

$$Cr(VI)O_{x,\,surf} + H_2O(g) \underset{\substack{\text{dry air}}}{\overset{\substack{800^\circ C}}{\rightleftarrows}} CrO_3 \overset{\substack{800^\circ C}}{\underset{\substack{\text{dry air}}}{\rightarrow}} Cr_2O_3 + O_2$$

(1)

$$Cr(III)O_{x,\,surf} + H_2O(g) \overset{\substack{800^\circ C}}{\underset{\substack{\text{dry air}}}{\rightarrow}} Cr_2O_3$$

(2)

on silica surface during the calcination process. The first route shown in Eq. (1) is a two-step process: at first, the chromate Cr(VI)O$_{x,\,surf}$ species is cleft by traces of moisture leading to the formation of CrO$_3$, and then the CrO$_3$ decomposes into Cr$_2$O$_3$. In this route, the first step is a reversible reaction and mainly goes to the Cr(VI)O$_{x,\,surf}$ side especially at low Cr loading and high temperature. This is supported by a mechanism proposed by Groeneveld et al. [14], Jóźwiak and Lana [18] that is traces of water vapor acts as a "promoter" for the stabilization of bulk chromium trioxide on the silica surface during the calcination process at high temperature as shown in Eqs. (3) and (4). The direct

$$CrO_3 + H_2O(g) \rightarrow CrO_2(OH)_2$$

(3)

$$CrO_2(OH)_2 + {\equiv}Si{-}OH_{surf} \rightarrow$$
$$Cr(VI)O_{x,\,surf} + H_2O(g)$$

(4)

$$CrO_3 + {\equiv}Si{-}O{-}Si{\equiv}_{surf} \rightarrow Cr(VI)O_{x,\,surf}$$

(5)

incorporation of bulk CrO$_3$ into the surface siloxane groups formed from dehydroxylation (shown in Eq. (5)) resulting in Cr(VI)O$_{x,\,surf}$ species at high temperature is also possible according to the reports

by McDaniel et al. [15], Jóźwiak and Lana [18]. So even if some $Cr(VI)O_{x, surf}$ species is occasionally cleft by traces of moisture leading to the formation of CrO_3, the later could be quickly re-anchored on the silica surface through the reaction with the neighboring hydroxyl or siloxane groups. Moreover, it is well known that the second step of the redox reaction (thermal decomposition of bulk CrO_3) can be efficiently suppressed by the presence of O_2 or dry air during calcination [4,43]. The occasional cleavage of $Cr(VI)O_{x, surf}$ species by traces of moisture is suggested to facilitate the migration and redispersion of $Cr(VI)O_{x, surf}$ species on the silica surface by Jóźwiak and Lana [18]. In the second route shown in Eq. (2), the supported $Cr(III)O_{x, surf}$ species is cleft by traces of moisture directly resulting in the formation of Cr_2O_3, which sounds more feasible due to its much less reversibility as well as no effect from the gas media(oxidizing or not) compared with the first route. In order to elucidate the origin and formation mechanism of the aggregated Cr_2O_3, the role of moisture in the formation of aggregated Cr_2O_3 during the calcination treatment of the Phillips catalyst is investigated in terms of calcination atmosphere (pure air or N_2). For getting more pronounced information, which would facilitate our judgement, extra moisture was purposely introduced into the gas media during the further calcination treatment of our catalyst sample. Substantially, the Phillips catalyst (S-1) in calcined form (800°C in dry air for 20 h) was further thermal-treated at 800°C for 2 h in moisture-contained pure air (S-2) and moisture-contained nitrogen (S-3) flow, respectively, before XPS and EPMA measurements. Different effects from oxidizing and non-oxidizing atmosphere during calcination shown in the first route (Eq. (1)) and the second route (Eq. (2)) could be expected and utilized to elucidate which route is in function.

The XPS spectra of Cr 2p level of S-2 and S-3 are shown in Fig. 1. The corresponding BE and FWHM values of Cr 2p(3/2) level obtained by multiplet fittings are listed in Table 2 together with those of S-1. For sample S-2 treated in moisture-contained pure air flow, two oxidation states were found namely the first with a BE of 581.64 eV and a FWHM of 8.30 eV assigned as an oxidation state of +6 (atomic concentration 59.4%) and the second with a BE of 577.58 eV and a FWHM of 3.28 eV assigned as an oxidation state of +3 (atomic concentration 40.6%). The first

can be ascribed to $Cr(VI)O_{x, surf}$ species based on previous discussion. About one-seventh of chromate $Cr(VI)O_{x, surf}$ species (i.e. ca. 10% of all surface Cr) in S-1 was reduced to the second Cr species in oxidation state of +3 after the treatment. The slightly decreased BE value of the $Cr(VI)O_{x, surf}$ species after treatment may be an indication of the preferential reduction of some specific $Cr(VI)O_{x, surf}$ species with the highest BE (corresponding to the lowest electron density and thus highest reduction-potential) on the silica surface during the treatment, while the effect from the variation of its neighborhood surrounding (e.g. the second Cr species) also cannot be ruled out. The FWHM value of the second Cr species is only 0.25 eV higher than that of bulk Cr_2O_3 measured in this work and almost the same as the average FWHM value of the bulk Cr_2O_3 calculated from the references [29,30,32,41] (shown in Table 1), so it is reasonable to assign this Cr species as bulk Cr_2O_3. As pointed out by Hercules et al. [35], sometimes it is difficult to judge the oxidation state of surface Cr species from the BE value due to its greater deviation than the FWHM, and the chemical shifts may be caused from the changes of both the atomic valence state and potential interaction with its environment. Here the chemical shift of the BE for the bulk Cr_2O_3 on S-2 towards higher position (contrary to the lower position of the pure bulk Cr_2O_3) can be rationalized by the explanation of its coexistence with the $Cr(VI)O_{x, surf}$ species on the silica surface. Moreover, this bulk Cr_2O_3 converted from the highly dispersed $Cr(III)O_{x, surf}$ and $Cr(VI)O_{x, surf}$ species by moisture most probably aggregated as dispersed micro-crystals covered on the chromate-rich areas (strong Lewis acids and much more electron-negative compared with the SiO_2 and Cr_2O_3) during the treatment. Consequently, the electron-releasing effect from the bulk Cr_2O_3 leads to its chemical shift to higher position. The above interpretation is favorably supported by the Best et al.'s report [31] on CrO_x/SiO_2 catalysts (300–600°C in air for 4 h) with 8 wt.% Cr loading. They found, when the bulk Cr_2O_3 coexists with chromate species (most probably also bulk CrO_3) on the catalysts calcined at lower temperature (300–400 °C), its BE lies between 577.4 and 577.5 eV, whereas when all the Cr species is converted into bulk Cr_2O_3 at higher temperature (500–600°C), then the BE decreases to 577.1 eV. Rahman et al. [26] investigated $CrO_x/alumna$ catalysts (500–800°C

in air for 24 h) with 5–15 wt.% Cr and found the BE of bulk Cr_2O_3 in mixed state with chromate species lies between 577.2 and 577.6 eV. According to XPS study of Cimino et al. [29], bulk Cr_2O_3 was found on Phillips CrO_x/SiO_2 catalysts (300–700°C in air for 5 h, 1–9 wt.% Cr) in mixture with chromate species at high Cr loading and/or high temperature, whereas it is very difficult to compare our XPS data with theirs due to the following reasons. Their curve fittings were just applied to the single Cr 2p(3/2) peak, and this might be at the risk of losing original information especially when the surface Cr species was in mixed oxidation states [28,42]. Moreover, they presented no BE and FWHM data except the final ratio of Cr(VI):Cr(III). For sample S-3 treated in moisture-contained N_2 flow, approximately the same results were obtained, that is two kinds of surface Cr species were found namely the first with a BE of 581.74 eV and a FWHM of 8.30 eV assigned as chromate species (atomic concentration 60.8%) and the second with a BE of 577.64 eV and a FWHM of 3.26 eV assigned as bulk Cr_2O_3 (atomic concentration 39.2%). It means all the $Cr(III)O_{x, surf}$ species (i.e. ca. 30% of all surface Cr) and about one-seventh of the $Cr(VI)O_{x, surf}$ species (i.e. ca. 10% of all surface Cr) was converted into bulk Cr_2O_3 in the presence of moisture upon the 800°C calcination for 2 h whatever pure air(oxidizing) or N_2 (neutral) was used. As illustrated in Table 2, the decrease of relative intensity of the Cr 2p level from 3.8 to 2.6 for S-2 and 2.7 for S-3 is also a reflection of the serious aggregation of Cr_2O_3 microcrystals [32]. Some part of the Cr_2O_3 microcrystals was surely beyond the XPS surface sensitivity restricted by the typical mean photoelectron escape depth of ca. 2 nm [35]. This is further clarified by the EPMA measurements. The EPMA map and line analysis of Cr distribution state reveals the highly aggregated Cr species on the S-2 and S-3 samples and the aggregation degree of surface Cr species is also similar for this two samples. Fig. 5 shows the EPMA map image and line curves of the S-2 sample. Besides many dispersed micro-particles in sizes of several 100 nm to several microns, which were supposed to be crystallized aggregates of Cr_2O_3, a few large aggregated Cr islands (marked in circles in Fig. 5(a) corresponding to the large peaks in Fig. 5(b)) were also found. The similar oxidation and distribution states of Cr on S-2 and S-3 samples obviously demonstrate that the formation of bulk Cr_2O_3
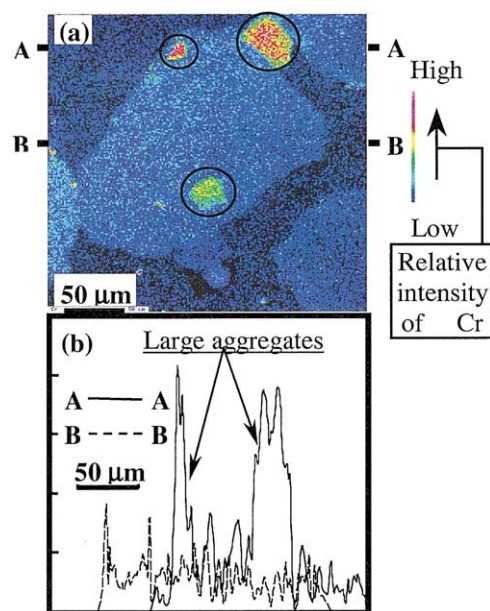

Fig. 5. The EPMA map (a) and line curves (b) of the chromium distribution on the sample (S-2) from treatment of S-1 in moisture-contained air flow at 800°C for 2 h. The line curves of A–A and B–B in (b) are corresponding to the chromium distribution at the straight-line positions of A–A and B–B in (a), respectively. The red and yellowish patches marked in circles in (a) are corresponding to large aggregates of surface Cr species.

is through the second route (Eq. (2)) rather than the first one(Eq. (1)), that is the supported $Cr(III)O_{x, surf}$ species is cleft by moisture directly resulting in the formation of Cr_2O_3. The $Cr(VI)O_{x, surf}$ species (ca. one-seventh of all $Cr(VI)O_{x, surf}$ species), which was converted into bulk Cr_2O_3 during the treatments, was also supposed to be firstly thermal-reduced into $Cr(III)O_{x, surf}$ species and then cleft by moisture due to the similar results between S-2 and S-3. Groeneveld et al. [14] studied the H_2-reduction (330–450°C) of a CrO_x/SiO_2 (500°C in air for 4 h) catalyst with ca. 0.37 Cr/nm^2. Before H_2-reduction, no decomposition into α-Cr_2O_3 was confirmed, whereas after reduction by H_2, the catalyst contains Cr^{2+} and Cr^{3+}, and the latter in various states of clustering. They postulated that the moisture formed in reduction reaction oxidizes the $Cr(II)O_{x, surf}$ to $Cr(III)O_{x, surf}$ species and hydrolyzes the monochromate or dichromate species into polychromate followed by the thermal-reduction of polychromate to Cr_2O_3. According to our experimental results and analysis, the thermal-reduction of
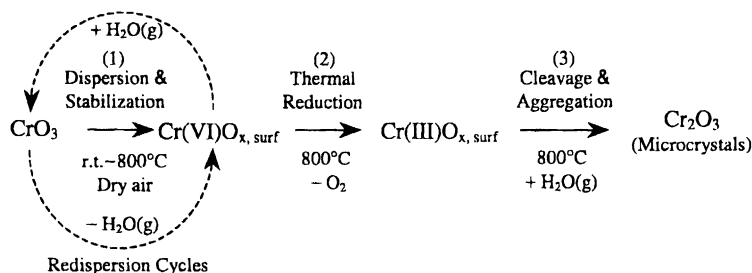
Scheme 1. Plausible mechanism of formation of aggregated Cr_2O_3 on the Phillips catalyst with 0.4 Cr/nm^2 during calcination in the preparation process.

chromate species (including polychromate) at such low temperature range (330–450°C) sounds unreasonable, and it would be much more acceptable to hypothesize that the Cr clustering in their H_2-reduced catalyst is originated from the interaction between the moisture and the $Cr(III)O_{x,\,surf}$ species.

3.3. Speculation on the formation mechanism of the aggregated Cr_2O_3

So far, a plausible mechanism concerning the formation of Cr_2O_3 microcrystals during calcination in the preparation process of the Phillips catalyst with an industrial level of Cr loading ca. 0.4 Cr/nm^2 can be speculated in Scheme 1. At the first stage (reaction (1) in Scheme 1.), the bulk CrO_3 is dispersed and stabilized as surface chromate species (i.e. monochromate and dichromate, sometimes even polychromate) through the reaction with the surface groups on silica during the calcination process from r.t. to 800°C in dry air. Gradually, a highly dispersed state of chromate species can be achieved through many redispersion cycles of sublimation, volatilization, spreading, deposition, and stabilization of bulk CrO_3, as well as hydrolysis, re-spreading, re-deposition and re-stabilization of chromate species on the support surface. These redispersion cycles may be facilitated by the presence of traces of moisture generating from the successive dehydroxylation of silica in the early stage of dispersing and supporting of bulk CrO_3 during calcination. During this period, the thermal decomposition of bulk CrO_3 can also be sufficiently inhibited by the presence of oxidizing gas(dry air or O_2). Gradually, the dehydroxylation also results in increasing strain in surface siloxane groups and thus increasing

reduction-potential of the surface chromate species. At certain critical point the calcination-induced reduction of chromate species to $Cr(III)O_{x,\,surf}$ species would be expected (reaction (2) in Scheme 1). Thereafter, further evolved traces of moisture from dehydroxylation might split some $Cr(III)O_{x,\,surf}$ species from silica surface leading to the formation of Cr_2O_3 microcrystals (reaction (3) in Scheme 1). Higher temperature, longer duration and higher content of moisture in the last stage of calcination process are sure to bring about more serious aggregation of surface Cr species. Further confirmation investigation of this mechanism assumption concerning the calcination in the preparation process of the Phillips catalyst is necessary and still in progress in terms of different calcination conditions especially in the earlier stage of calcination. The results will be available for publication later soon.

4. Conclusions

The physico-chemical state and aggregation mechanism of surface Cr species on an industrial Phillips CrO_x/SiO_2 catalyst calcined in dry air at 800°C for 20 h with 0.4 Cr/nm^2 Cr loading are investigated by the combined techniques of XPS and EPMA. Firstly, a clear image of the physico-chemical state of surface Cr species on the catalyst is obtained, that is the co-existence of three kinds of surface Cr species on the catalyst surface namely the $Cr(VI)O_{x,\,surf}$ (ca. 70%) and $Cr(III)O_{x,\,surf}$ species (ca. 29%) and small amount of aggregated Cr_2O_3 microcrystals. Consequently, the calcination-induced reduction of $Cr(VI)O_{x,\,surf}$ to $Cr(III)O_{x,\,surf}$ species as well as the formation of Cr_2O_3 microcrystals in a calcined Phillips catalyst

with relatively low Cr loading were specifically confirmed. Further investigation is focused on the origin and formation mechanism of this aggregated Cr_2O_3 microcrystals. The role of moisture in the formation of aggregated Cr_2O_3 during the calcination treatment of the catalyst is studied in terms of calcination atmosphere (pure air or N_2), in which extra moisture was introduced for getting more pronounced information. Substantially, the Phillips catalyst (S-1) was further thermal-treated at $800°C$ for 2 h in moisture-contained pure air (S-2) and moisture-contained nitrogen (S-3) flow, respectively, before XPS and EPMA measurements. It was found that the purposely introduced moisture induced the transformation of all the $Cr(III)O_{x,surf}$ species and one-seventh of the $Cr(VI)O_{x,surf}$ species into aggregates of Cr_2O_3 at high temperature in this two samples without any obvious difference generated between using the oxidizing and inert atmosphere. Finally, the formation mechanism of aggregated Cr_2O_3 microcrystals induced by traces of moisture through cleavage of the $Cr(III)O_{x,surf}$ species during the calcination had been speculated considering of the indispensable evolution of traces of moisture from the simultaneous dehydroxylation of residual hydroxyl groups on silica surface.

Acknowledgements

References

[1] A. Clark, Catal. Rev. 3 (1970) 145.
[2] Y. Yermakov, V. Zakhrov, Adv. Catal. 24 (1975) 173.
[3] J. Boor, Ziegler–Natta Catalysts and Polymerization, Academic Press, New York, 1978, p. 279.
[4] M. McDaniel, Adv. Catal. 33 (1985) 47.
[5] A. Guyot, R. Spitz, in: R.B. Seymour, T. Cheng (Eds.), History of Polyolefins, Reidel, Holland, 1986, p. 271.
[6] F.J. Karol, S.C. Kao, New J. Chem. 18 (1994) 97.
[7] C.E. Marsden, Plast. Rubber Compos. Process. Applic. 21 (1994) 193.
[8] B.M. Weckhuysen, I.E. Wachs, R.A. Schoonheydt, Chem. Rev. 96 (1996) 3327.
[9] B.M. Weckhuysen, R.A. Schoonheydt, Catal. Today 51 (1999) 215.
[10] H. Charcosset, A. Revillon, A. Guyot, J. Catal. 8 (1967) 326.
[11] H. Charcosset, A. Revillon, A. Guyot, J. Catal. 8 (1967) 334.
[12] A. Guyot, H. Charcosset, A. Revillon, G. Vuillaume, J. Macromol. Sci. Chem. A2 (1968) 135.
[13] H. Charcosset, A. Revillon, A. Guyot, J. Catal. 9 (1967) 295.
[14] C. Groeneveld, P.P.M.M. Wittgen, A.M. Van Kersbergen, P.L.M. Mestrom, C.E. Nuijten, G.C.A. Schuit, J. Catal. 59 (1979) 153.
[15] M.P. McDaniel, J. Catal. 67 (1981) 71.
[16] S. Wang, K. Murata, T. Hayakawa, S. Hamakawa, K. Suzuki, Appl. Catal. A: Gen. 196 (2000) 1.
[17] M.A. Vuurman, F.D. Hardcastle, I.E. Wachs, J. Mol. Catal. 84 (1993) 193.
[18] W.K. Jozwiak, I.G.D. Lana, J. Chem. Soc., Faraday Trans. 93 (1997) 2583.
[19] A. Ellison, T.L. Overton, L. Bencze, J. Chem. Soc., Faraday Trans. 89 (1993) 843.
[20] A. Bensalem, B.M. Weckhuysen, R.A. Schoonheydt, J. Chem. Soc., Faraday Trans. 93 (1997) 4065.
[21] A. Ellison, J. Chem. Soc., Faraday Trans. 80 (1984) 2567.
[22] M.I. Zaki, N.E. Fouad, J. Leyrer, H. Knozinger, Appl. Catal. 21 (1986) 359.
[23] F.D. Hardcastle, I.E. Wachs, J. Mol. Catal. 46 (1988) 173.
[24] M. Richter, P. Reich, G. Ohlmann, J. Mol. Catal. 46 (1988) 79.
[25] A. Ellison, G. Diakun, P. Worthington, J. Mol. Catal. 46 (1988) 131.
[26] A. Rahman, M.H. Mohamed, M. Ahmed, A.M. Aitani, Appl. Catal. A: Gen. 121 (1995) 203.
[27] H. Schmidt, W. Riederer, H.L. Krauss, J. Prakt. Chem. 338 (1996) 627.
[28] J.R. Sohn, S.G. Ryu, Langmuir 9 (1993) 126.
[29] A. Cimino, B.A. De Angelis, A. Luchetti, G. Minelli, J. Catal. 45 (1976) 316.
[30] Y. Okamoto, M. Fujii, T. Imanaka, S. Teranishi, Bull. Chem. Soc. Jpn. 49 (1976) 859.
[31] S.A. Best, R.G. Squires, R.A. Walton, J. Catal. 47 (1977) 292.
[32] R. Merryfield, M. McDaniel, G. Parks, J. Catal. 77 (1982) 348.
[33] A. Cimino, D. Cordischi, S.D. Rossi, G. Ferraris, D. Gazzoli, V. Indovina, G. Minelli, M. Occhiuzzi, M. Valigi, J. Catal. 127 (1991) 744.
[34] D. Gazzoli, M. Occhiuzzi, A. Cimino, G. Minelli, M. Valigi, Surf. Inter. Anal. 18 (1992) 315.
[35] D.M. Hercules, A. Proctor, M. Houalla, Accounts Chem. Res. 27 (1994) 387.
[36] B.M. Weckhuysen, A.A. Verberckmoes, A.L. Buttiens, R.A. Schoonheydt, J. Phys. Chem. 98 (1994) 579.
[37] I. Hemmerich, F. Rohr, O. Seiferth, B. Dillmann, H.J. Freund, Zeitschrift Fur Physikalische Chemie, Int. J. Res. Phys. Chem. Chem. Phys. 202 (1997) 31.
[38] P.C. Thüne, C.P.J. Verhagen, M.J.G. van den Boer, J.W. Niemantsverdriet, J. Phys. Chem. 101 (1997) 8559.

[39] D.H. Cho, S.D. Yim, G.H. Cha, J.S. Lee, Y.G. Kim, J.S. Chung, I.S. Nam, J. Phys. Chem. 102 (1998) 7913.

[40] Q. Xing, W. Milius, H.L. Krauss, Z. Anorg. Allg. Chem. 625 (1999) 521.

[41] G.C. Allen, M.T. Curtis, A.J. Hooper, P.H. Tucker, J. Chem. Soc., Dalton Trans., 1675 (1973).

[42] A. Cimino, D. Cordischi, S. De Rossi, G. Ferraris, D. Gazzoli, V. Indovina, G. Minelli, M. Occhiuzzi, M. Valigi, J Catal. 127 (1991) 744.

[43] M.P. McDaniel, J. Catal. 76 (1982) 37.

[44] K.G. Miesserov, J. Polym. Sci.: A-1 4 (1966) 3047.

[45] B.M. Weckhuysen, I.E. Wachs, J. Phys. Chem. B 101 (1997) 2793.

[46] L.M. Baker, W.L. Carrick, J. Org. Chem. 35 (1970) 774.

[47] J.P. Hogan, J. Polym. Sci.: A-1 8 (1970) 2637.

[48] D.L. Kim, J.M. Tatibouet, I.E. Wachs, J. Catal. 136 (1992) 209.

[49] M.A. Vuurman, I.E. Wachs, D.J. Stufkens, A. Oskam, J. Mol. Catal. 80 (1993) 209.

[50] D.L. Kim, I.E. Wachs, J. Catal. 142 (1993) 166.

[51] B. Fubini, G. Ghiotti, L. Stradella, E. Garrone, C. Morterra, J. Catal. 66 (1980) 200.

[52] K. Hasebe, H. Mori, M. Terano, J. Mol. Catal. A: Chem. 124 (1997) L1.

[53] H. Mori, K. Hasebe, M. Terano, J. Mol. Catal. A: Chem. 140 (1999) 165.

[54] H. Mori, K. Hasebe, M. Terano, Polymer 40 (1999) 1389.

[55] H. Mori, M. Terano, in; T. Sano, T. Uozumi, H. Nakatani, M. Terano (Eds.), Progress and Development of Catalytic Olefin Polymerization, Technology and Education Publishers, Tokyo, 2000, p. 280.

[56] K. Hasebe, H. Mori, M. Tomotori, T. Keii, M. Terano, J. Mol. Catal. A: Chem. 115 (1997) 259.

[57] H. Mori, K. Hasebe, M. Terano, Macromol. Chem. Phys. 199 (1998) 2709.